

DESIGN AND EVALUATION OF AN ENERGY MANAGEMENT SYSTEM APPLIED TO A LOWER LIMB ROBOTIC EXOSKELETON

MIGUEL MENDIETA¹, CRISTIAN MUNOZ¹, L. G. GONZALEZ¹, HUIYAN ZHANG²
AND LUIS I. MINCHALA¹

¹Department of Electrical Electronics and Telecommunications Engineering
University of Cuenca
Ave. 12 de Abril y Agustin Cueva, Cuenca, Ecuador
{miguel.mendieta; cristian.munoz; luis.gonzalez; ismael.minchala}@ucuenca.edu.ec

²National Research Base of Intelligent Manufacturing Service
Chongqing Technology and Business University
No. 19, Xuefu Avenue, Nan'an District, Chongqing 400067, P. R. China
huiyanzhang@ctbu.edu.cn

Received October 2020; revised February 2021

ABSTRACT. *This paper presents the design, development and evaluation of an energy management system (EMS) for covering the energy demand from an autonomous lower limb exoskeleton (ALLEX) prototype. The ALLEX prototype is composed by four energy subsystems: actuators, sensing, communications, and control. The energy demanded by ALLEX is estimated by considering metabolic requirements of neurological rehabilitation applied to the actuators subsystem, as well as average consumption of the sensing, communications, and control subsystems. The EMS proposed in this paper is composed by a lithium-ion battery bank, a battery management system (BMS), and proper instrumentation for measuring voltages, currents, and temperature from the battery pack. Experimental results show adequate coverage of the energy demand from ALLEX, both instantly and during continuous operation (1 hour approximately). Additionally, the efficiency of the EMS is assessed by testing the cells balancing and battery charging/discharging processes, which showed equalized values of the energy cells as well as correct temperature operating values.*

Keywords: Batteries, Battery management system, Cells balancing, Lower limb robotic exoskeleton, Energy management system

1. **Introduction.** Nowadays, the impact of technology on people's quality of life is most evident in applications related to the field of health. For instance, robotic exoskeletons are devices designed to assist users' mobility in various application areas, including:

- Neurological rehabilitation, involving assistance in the mobility of the joints and/or limbs of patients with limited functionality;
- Military and industrial applications through assistance in repetitive handling movements of large and heavy objects.

The interaction between these devices and users is carried out through bio-metric signal processing systems, which regulate actuator's speed and position of each joint in order to meet specific tasks [1, 2]. These interaction systems provide autonomy in the operation of the device when a patient uses the robotic exoskeleton [3]. Several studies about robotic exoskeletons demonstrate their advantages [4, 5, 6], among which, are their high accuracy of movements, adaptability to the user needs, and portability.

The mobility aids provided by these devices operate in two ways: i) passively, using the patient's potential and kinetic energy, and ii) actively, through energy storage systems. The use of electrochemical storage systems is common, due to its safety characteristics and energy density. However, there are few studies related to the energy management of robotic exoskeletons, which is a vital aspect due to the portable nature of this equipment [7]. In this context, for instance, extending the autonomy of operation by using large batteries implies an increase of weight of the equipment, as well as the necessity of larger space for installing the battery cells [8]. One of the main challenges when designing energy storage systems (ESS) is related with the harmonization of operating parameters, such as state of charge, temperature, charge and discharge currents, and cells balancing, which typically are managed by an EMS [9]. The correct selection, configuration and programming of an EMS related to lower limb robotic exoskeletons has been hardly reported in formal literature and is deeply discussed throughout this paper by showing integration methodologies and experimental results.

Electrochemical batteries are the most widely used electrical energy storage devices in mobile and portable equipment. The main application niche of this technology corresponds to mobile telephony and electric vehicles [10]. However, this storage technology presents disadvantages during its operation due to the continuous use and the repeated charge/discharge cycles, affecting its duration and energy storage capacity [11]. To reduce the degradation and performance process of batteries during periods of charge and discharge, it is necessary to have systems that regulate the operating conditions by continuously monitoring voltage, current and temperature [12].

This paper presents the design, implementation and experimental evaluation of an energy management system applied to an autonomous lower limb exoskeleton (ALLEX), consisting of six degrees of freedom (one actuator per joint). The energy management system integrates a bank of lithium-ion batteries with a BMS, which allows the monitoring of variables of interest in continuous charging and discharging operation cycles, in addition to managing the load balancing of the battery bank. Experimental tests applied to the prototype show efficiency during operation, highlighting the charge balancing process, real-time monitoring of voltages, currents, and temperatures, as well as the coverage of the energy demand of the robotic exoskeleton.

This paper is organized as follows: Section 2 presents design details of the energy management system applied to the lower limb robotic exoskeleton. Section 3 presents details of the implementation of the power system. Section 4 presents experimental results of the energy system operating under conditions of cell charge, discharge and balancing. Section 5 presents the conclusions of the work.

2. Energy Management System Applied to Lower Limb Robotic Exoskeleton.

2.1. Estimation of energy consumption during biped walking. Any movement that the human body executes demands metabolic energy. The use of exoskeletons requires quantifying this energy to assist and/or replace limb movements. References [13, 14] report the body's energy consumption in an approximate way, for various conditions. For instance, a person while resting, has active basal metabolism, or basal energy expenditure, which approximates 44 W/m^2 for men and 41 W/m^2 for women¹.

A biped walk of a person transporting a 10 kg load represents an average energy consumption of 185 W/m^2 , including the basal energy expenditure. Therefore, the metabolic

¹These values correspond approximately to the basal metabolism of a man of 1.70 m, 70 kg and 35 years of age, and of a woman of 1.60 m, 60 kg and 35 years of age.

energy dedicated exclusively to physical effort is 218.9 kcal/h and 254 W of instantaneous power.

The energy estimation for the ALLEX prototype starts by considering the work developed by authors of [15], who use a set of mechanical actuators from the Maxon motors brand to build a lower limb robotic exoskeleton composed by three actuators, as follows:

- Hip actuator. EC90 flat motor (90 W of nominal power).
- Knee actuator. EC45 flat motor (70 W of nominal power).
- Ankle actuator. EC45 flat motor (70 W of nominal power).

This design is similar to the prototype used in this study, so it is used as reference for calculating power requirements for the actuators. In this sense, the set of 3 electrical motors used for each leg (6 actuators in total) provides a nominal power for movement assistance of 460 W; additionally, considering an energy efficiency of the motors under study, close to 85%, the available mechanical power is 391 W. According to [4] the torque exerted by the joints during the dynamic regime is not constant at nominal power values; for example, the knee joint remains constant during the majority of the walk cycle. Therefore, the energy expenditure during the walk involves approximately 70% of the nominal power of mechanical systems. This implies a demand for mechanical power on axis, close to 273 W, which corresponds to a power slightly higher than that calculated by the metabolic analysis, which will allow a full energy coverage of the energy system during continuous use of the prototype.

2.2. Design of the energy system for the lower limb robotic exoskeleton. The energy consumption of the robotic exoskeleton involves the energy needs described in the previous Section 2.1, in addition to the energy requirements from the sensor, communications and control subsystems. Figure 1 shows a conceptual diagram of the main components of the proposed energy system. The energy management system involves a set of power converters that supply energy to the exoskeleton subsystems, as described in Table 1. The energy expenditure of the main subsystems in Figure 1 is detailed in Table 1. The first column shows the maximum consumption of the components, while the second column shows the average consumption, representing 70% of the maximum consumption.

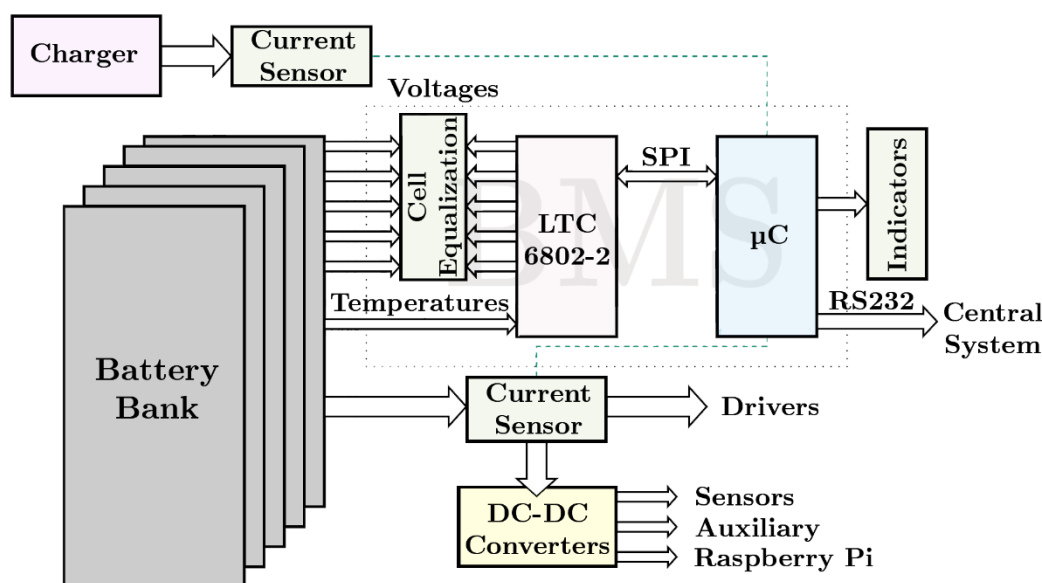


FIGURE 1. Proposed energy system for the lower limb robotic exoskeleton

TABLE 1. Electrical energy from exoskeleton subsystems

Devices	Maximum power	Average power
Actuators	460 W	322 W
DC-DC converter (Raspberry)	12.5 W	8.75 W
DC-DC converter (Drivers)	7 W	4.9 W
DC-DC converter (Sensors)	9 W	6.3 W
DC-DC converter (Auxiliary)	5 W	5 W*
μ C LTC6802-2	1.5 W	1.5 W*

*This equipment shows equal energy consumption since they are auxiliary devices installed in the system, such as a tactile screen, and microcontrollers, which are independent of the walking cycle.

The functionalities of the exoskeleton energy subsystems are described below.

- Actuators subsystem. This subsystem manages the energy of the actuators and regulates the position of the exoskeleton through distributed controllers which consist of brushless DC motor drivers and position sensors.
- Sensors subsystem. This subsystem supplies power to all signal conditioning circuits, which involves position sensors, EMG signals, and variables related to power management, which include hall effect current and voltage sensors.
- Communications subsystem. Manage the energy demand from the communication modules within the prototype, visual indicators of the state of operation and graphical human-machine interfaces (HMI).
- Control subsystem. Regulate the routines of coordination of the movement of the exoskeleton. This subsystem is mainly composed of a Raspberry Pi 3B+. Additionally, the energy of this subsystem is used to energize the EMS, consisting of a microcontroller and the circuit dedicated to the equalization and processing of variables associated with the battery bank.

The energy storage system is composed by a set of series-connected cells. The cells are lithium-ion with an iron phosphate cathode (LiFePO₄) which have specific power and energy of 5200 W/kg and 126 Wh/kg, respectively, and a life cycle greater than the 1000 cycles. The set of cells used corresponds to 20 Ah Prismatic Pouch Cell, UltraPhosphate™ Lithium-Ion model. Due to the series configuration, they tend to suffer imbalances throughout different charging cycles. These imbalances result in reduced battery bank overall performance and lifetime. To counteract against these imbalances, there are techniques designed to prevent this degradation, e.g., BMS circuits that are mainly responsible for mediating and balancing the state of charge and voltage of each cell, cycle charging/discharging of the cells, generally made up of a series of devices in charge of monitoring the cells, voltages, temperatures, etc., for their analysis and control [11].

The operation of the BMS depends on reliable measurements of the cells parameters, so devices that produce or enter the least possible error are required in order to calculate the state of charge (SoC) of the battery [16]. Many research works focus on the study of the batteries SoC since it is an important factor affecting the battery management system performance [17]. One of the circuits dedicated to this measurement, and the one used in this study, is the LTC6802-2, which is an integrated circuit (IC) designed to operate as a BMS, capable of measuring up to 12 cells with a total voltage of 60 V and with a maximum of 0.25% error in measurement; it also has input ports for thermistors to allow temperature measurement from the cells.

As stated before, the battery management is developed by the IC LTC6802-2, which executes important tasks to guarantee the correct operation of the energy system. Figure 2 shows main functionalities of the BMS. A short description of every functional block is as follows.

- The *measurement* module is responsible for the acquisition of variables such as voltage, current and temperature from the battery cells. The sampling time configured for this prototype is 0.5 s.
- The *SoC estimation* module uses the nominal capacity, estimated from the voltage and current of the battery bank, to calculate the state of charge of the battery pack.
- The *SoH estimation* module is not configured for this prototype. Nevertheless, this module is able to estimate the state of health of the batteries by using parameters related to the performance and time of use of the battery bank; typically, SoH estimation techniques are based on measurements of resistance and internal conductance, capacity, or the count of the number of charge and discharge cycles [18].
- The *capacity estimation* module estimates the capacity under current usage conditions. This estimation is used by the SoH estimation module.
- The *thermal management* module takes actions depending on the temperature of the cells to restrict the charge or discharge current in the battery bank and/or to regulate cooling systems. In this study, thermal management is limited only to the sensing of the battery bank and the management of over-temperature indicators.
- The *cell balancing* or equalization of the battery bank deals with the degradation present in the battery cells, which could represent uneven behavior, and progressively reduce the battery bank life. The equalization consists of balancing the cell voltages,

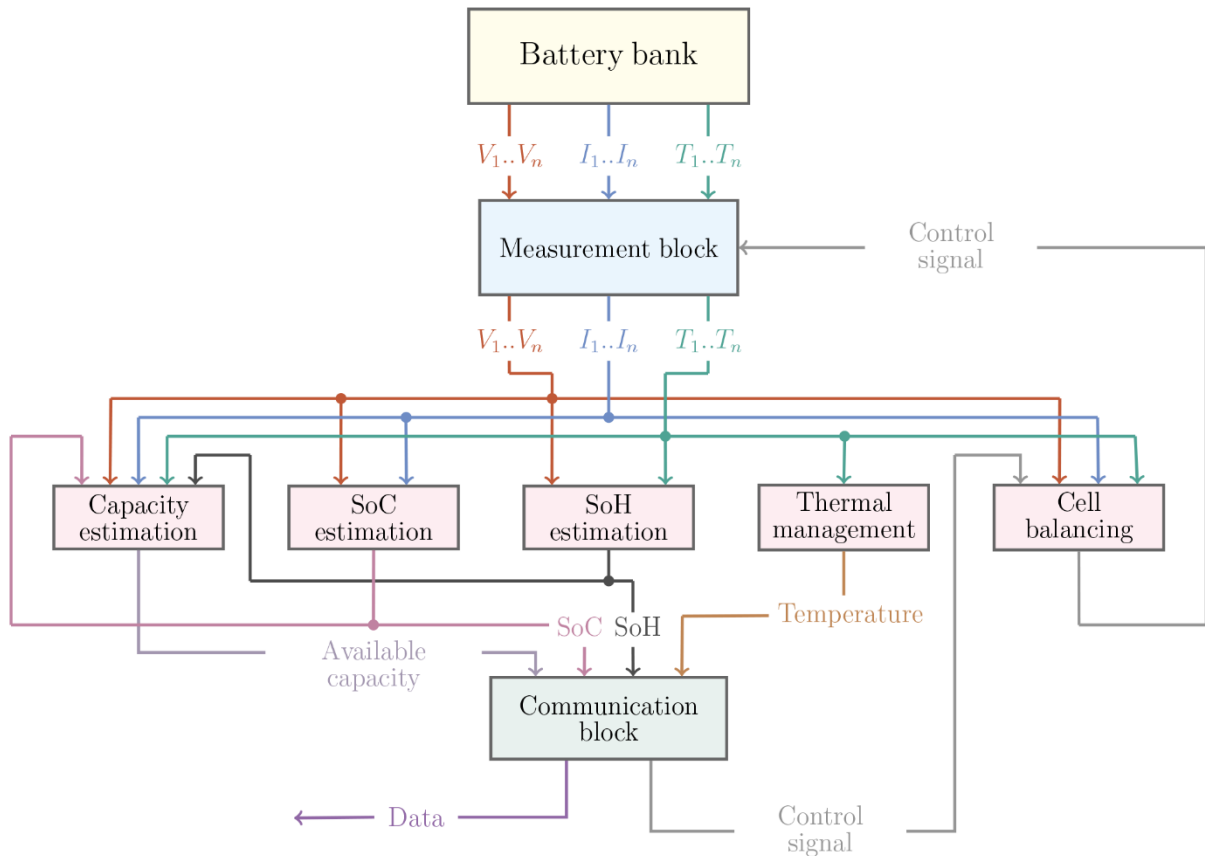


FIGURE 2. BMS function modules

this action that can be carried out mainly by two techniques: i) passive balancing consisting of discharging all cells except one, until the cell voltage with the lowest voltage is reached, and ii) active balancing, which transmits energy from the cell with the highest voltage to the one with the lowest value, preventing waste.

- The *communication* module is in charge of communicating the BMS with the external control units using CAN, SPI, I2C and RS232 protocols.

3. Implementation of the Energy Management System. The energy capacity of the energy system proposed in this study is calculated from the previous estimation of the average energy consumption, $P_{exo} = 348.45 \text{ W}^2$, and an autonomy of 1 hour of continuous use. From this autonomy, at least a capacity of 348.45 Wh is required. Considering a minimum charge state of 15%, a storage capacity greater than 409.94 Wh is necessary, with a nominal voltage of 24 V @ 17.08 Ah. For this amount of energy, 8 series-connected cells have been used, each one of the 20 Ah Prismatic Pouch Cell, with a nominal voltage of 3.3 V. As previously mentioned, the LTC6802-2 IC equalizes the battery cells by using a passive balancing. The balancing or equalization of the cells is carried out when there is a difference greater than 0.1 V with respect to the cell with the lowest voltage, and is maintained until the cell voltage is reduced to a difference of 0.01 V.

Charge and supply currents are measured using ACS712 current sensors; in addition, there are 2 NTC temperature sensors, managed by the LTC6802-2, which has 12-bit A/D converters, whose input signals are fed through signal conditioning circuits. The EMS is controlled by an Arduino nano microcontroller, which communicates with the IC LTC6802-2 via SPI protocol.

Figure 3 shows a flow diagram of the system operation routine. At first, the Arduino microcontroller initializes the LTC6802-2 registers, which are then set with current, voltage and temperature measurements. The current measurement is performed by the ACS712 sensor. According to the voltage of every cell from the battery bank (V_i ; $i = 1, 2, \dots, 8$), the microcontroller performs the following tasks:

- Determine the cell with the lowest voltage (V_{low});
- Calculate the voltage difference of every cell with respect to V_{low} , i.e., $\Delta V_i = V_i - V_{low}$ for $i = 1, 2, \dots, 8$;
- $\exists \Delta V_i \geq 0.01 \text{ V} \rightarrow$ The cell equalization operation is initiated and remains operative until $\Delta V_i < 0.01 \text{ V}$.

At the end, the LTC6802-2 registers are updated with current measurements, and the whole process starts over.

Figure 4 shows the prototype of the portable power system to be installed in the robotic exoskeleton. The labels allow to identify the subsystems presented in the system design.

4. Experimental Results. The BMS allows managing the charge/discharge cycles of the cells of the battery bank. Experimental analysis of the prototype operation involves verification of load balancing and tests related to the storage capacity of the battery bank, including thermal behavior.

4.1. Cell balancing on the battery bank. To verify the theoretical design and identify problems, that potentially arise in the operation of the system, the cells of the bank, composed by 8 lithium-ion batteries, are precharged at different voltages to verify the behavior of the load balancing system.

²This quantity is obtained by summing up the values shown in Table 1.

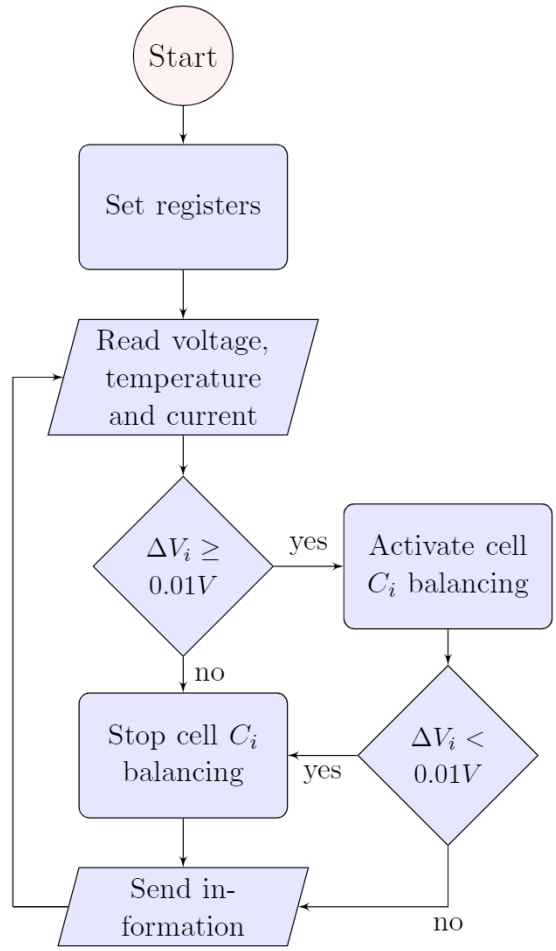


FIGURE 3. BMS operation flow chart

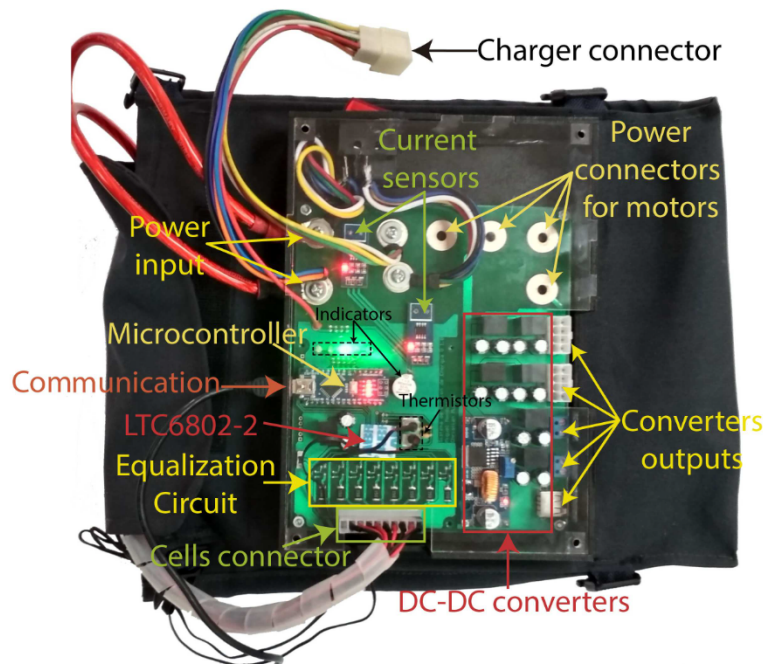


FIGURE 4. Prototype of the energy management system

Experimental tests of this stage involve the following two studies:

- Case 1. The voltage difference with respect to the lower cell voltage is $\Delta V_{\max_case1} = 0.035$ V;
- Case 2. The voltage difference with respect to the lower cell voltage is $\Delta V_{\max_case2} = 0.452$ V.

The total error in the cell voltage measurement was less than 1.5 mV. This deviation is acceptable for purposes of error detection and monitoring of battery charge. Table 2 shows the cell voltage in the initial and final state of the two study cases.

TABLE 2. Initial and final voltages in case of study

	Cell	1	2	3	4	5	6	7	8
Case 1	V_{ini}	3.568	3.574	3.576	3.579	3.583	3.572	3.559	3.548
(8.2 h)	V_{end}	3.558	3.558	3.558	3.558	3.558	3.558	3.558	3.558
Case 2	V_{ini}	3.132	3.471	3.482	3.385	3.572	3.125	3.340	3.462
(37.5 h)	V_{end}	3.132	3.132	3.132	3.132	3.132	3.132	3.132	3.132

Figure 5 shows the transient response of the charge balancing in the cells of the battery bank for the two study cases. Figure 5(a) shows a maximum differential voltage of $\Delta V_{\max_case1} = 0.035$ V, and for case 2, Figure 5(b) shows a maximum differential voltage of $\Delta V_{\max_case2} = 0.452$ V, corresponding to the preloaded values for these tests. The equalization duration for these experiments were 8.2 h and 37.5 h for the first and second cases, respectively. It is important to note that the voltage in the cells under the equalization process is reduced simultaneously, until the threshold $\Delta V = 0.01$ V is reached.

The equalization process runs by default as long as the battery bank reaches the minimum operating voltage, and can be run during the battery charging process and/or during use of the power system. The initial behavior of Figure 5(b), corresponds to an atypical case, given that the imbalance present in the bank cells is high (13.5% of the nominal voltage) and in turn the equalization time is equally long. The EMS detects imbalances higher than 0.01 V and starts the equalization process avoiding long balancing times.

4.2. Battery bank cell charging. The energy system prototype proposed in this study uses the PB-360P-24 battery charger for the charging process. In order to evaluate the behavior during this process, the cells were loaded from the voltages shown in Table 3.

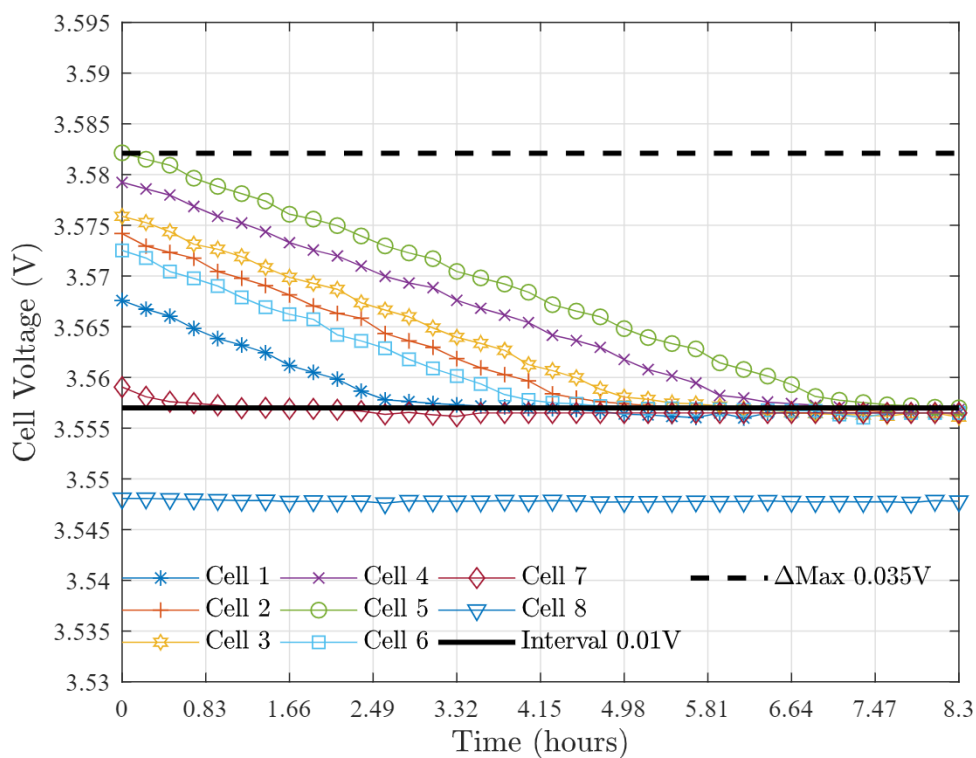
The performance of the partial charge process using the PB-360-24 charger, and with the operation of the EMS is shown in Figure 6. The initial voltages correspond to those in Table 3. During the charging process, the following stages are identified:

- Charging starts in constant current mode;
- Continuous charging in constant voltage mode; and,
- End of charge and start of floating mode.

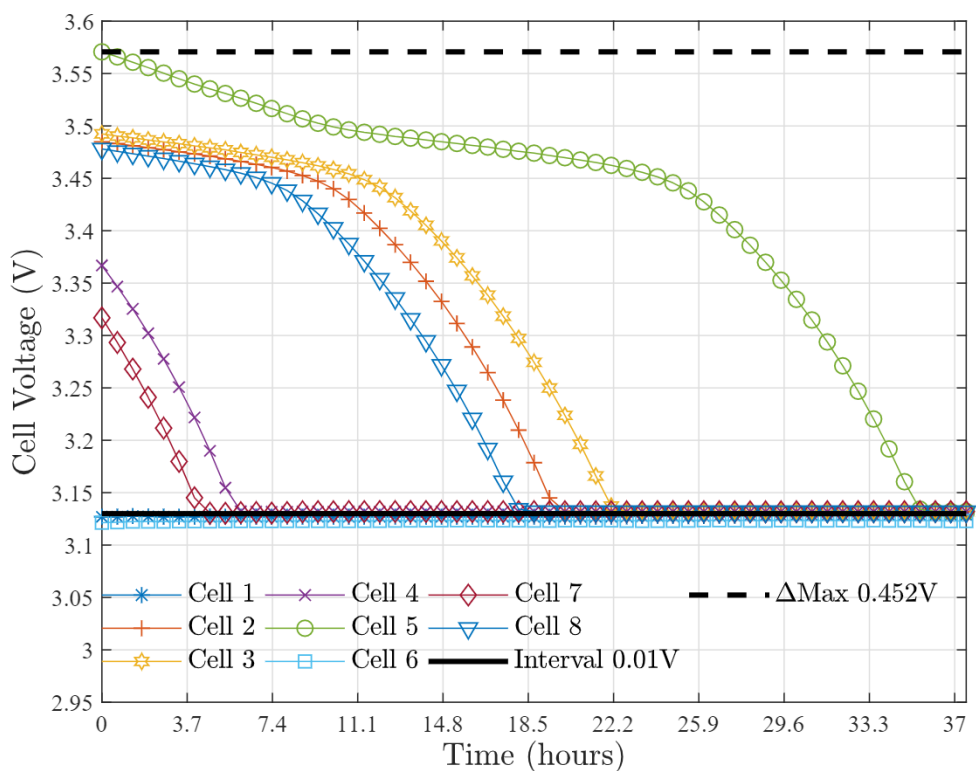
During the first, constant current, stage, the supply is 12.5 A for approximately 8 min; then the charging process is performed with constant voltage during 55 minutes until the charge is complete.

At the end of the partial charge process, it is observed that the equalization system reduces the difference in voltages present in the charging process, allowing the homogeneous behavior of the cells of the battery bank.

For the study of the battery bank storage capacity and the energy performance of the storage system, Figures 7(a) and 7(b) show the behavior of the variables of interest during the charging and discharging of the battery bank. In a full charge process at a charge rate less than 0.2C, a battery bank voltage of 31.32 V and a marginal current of 500 mA are



(a) Voltage of the equalization process (case 1)



(b) Voltage of the equalization process (case 2)

FIGURE 5. Equalization process

TABLE 3. Initial cell voltage in charging process

Cell	1	2	3	4	5	6	7	8
Voltage	3.218	3.207	3.232	3.219	3.224	3.219	3.227	3.276

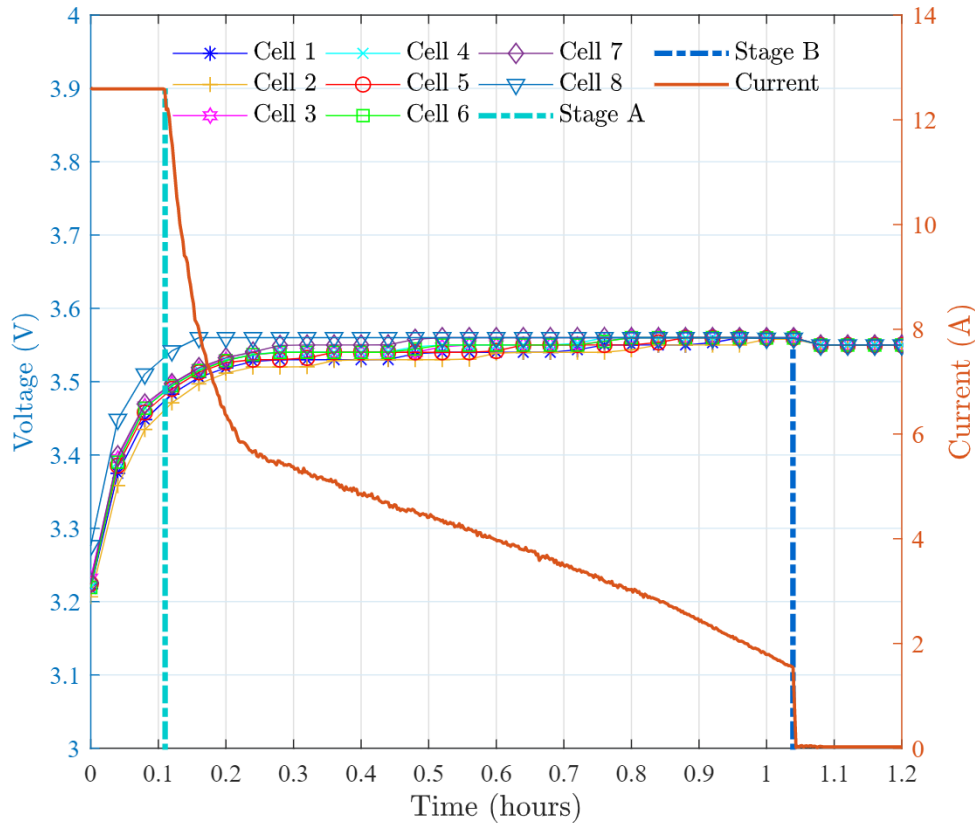


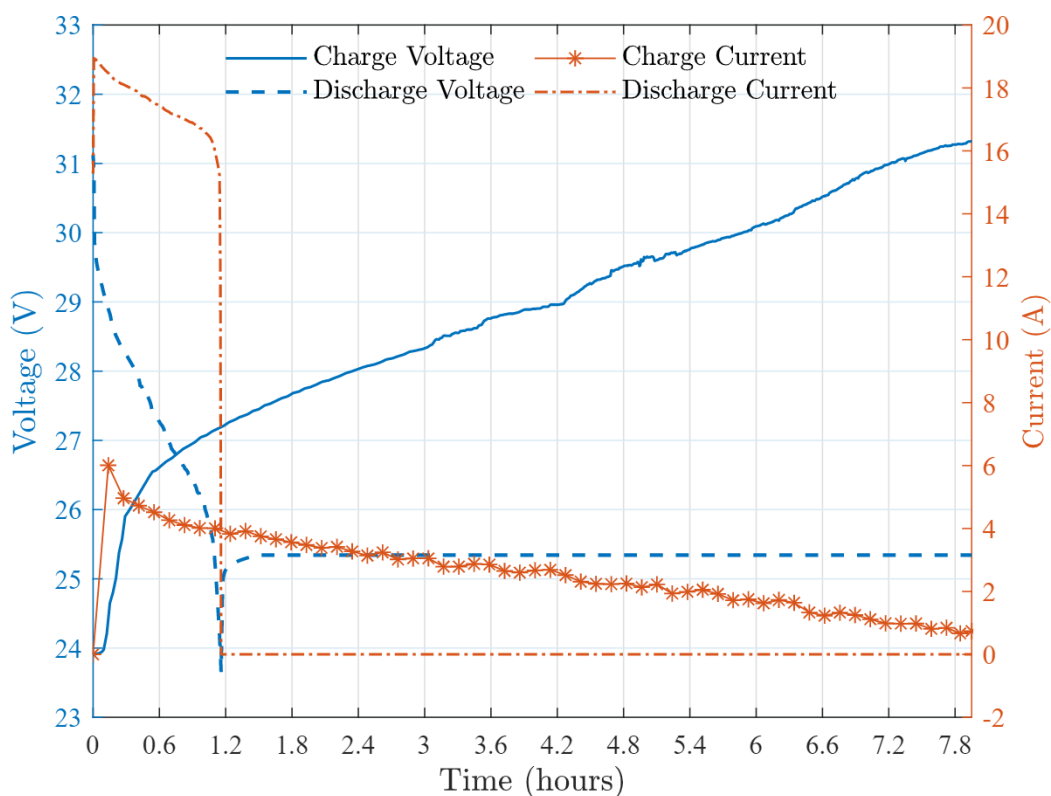
FIGURE 6. Behavior in partial charge process

initially reached at 7.95 h. In this charging process the bank absorbs an electric charge of 20.70 Ah, and an energy of 612 Wh.

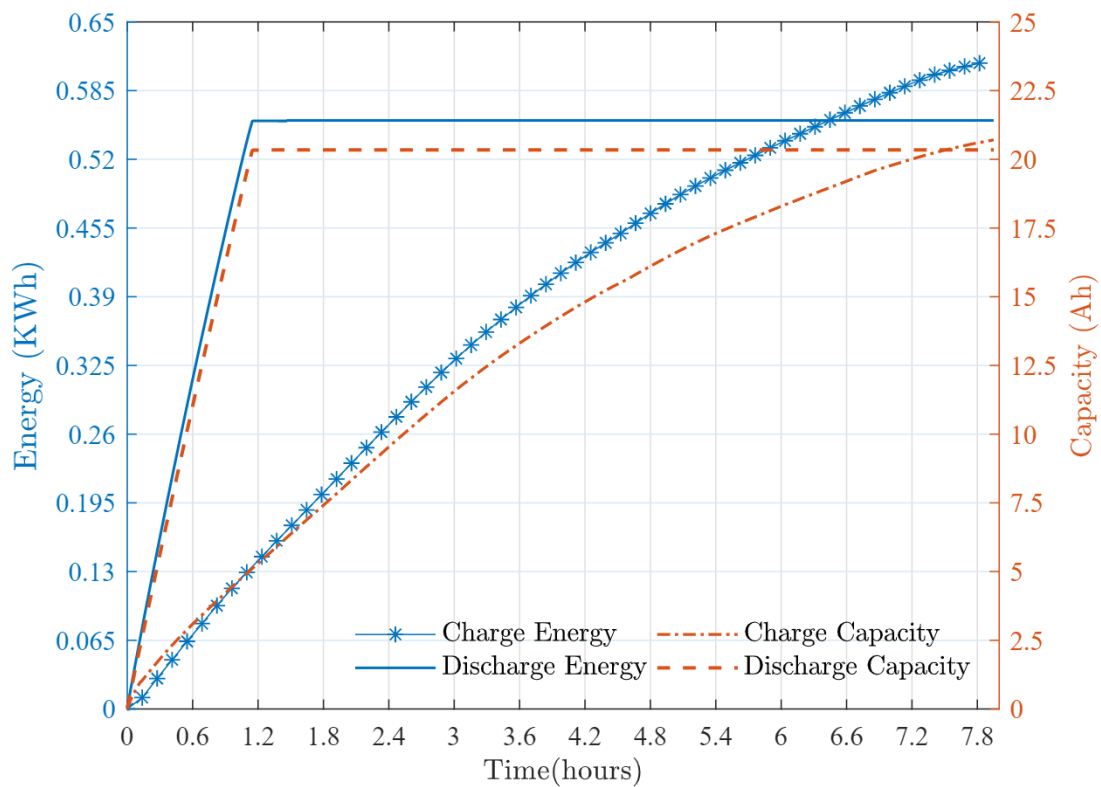
The battery bank discharge process is performed at approximately a rate of 1C, using a resistive load of 1.7Ω . Figure 7(a), shows the voltage of the battery bank during discharge, with an approximate duration of 70 min, initial current of 19 A and final current of 15 A. The initial voltage of the battery bank is 31.13 V and the final discharge is 23.65 V supplying an electric charge of 20.34 Ah and an energy of 557.26 Wh in 1.15 h. The performance obtained from the energy storage cycle shows a performance of 91.05%, which is consistent with the storage technology used.

Finally, the thermal behavior during the discharge at a rate of 1C, is synthesized in Figure 8. The thermal behavior of the sensors located at the middle and at the border of the cells of the battery bank shows an increase of 5°C in temperature at the end of the discharge process, this variation is within the range allowed by the manufacturer (-30°C @ 55°C), and consequently, the BMS guarantees that there is no risk of overheating under normal operating conditions.

5. Conclusions. The energy system proposed in this research supplies energy in a portable way to a prototype of a lower limb robotic exoskeleton. The main component of the system is the integrated circuit LTC6802-2 IC, which manages a set of power



(a) Voltage and current behavior in full charge and discharge



(b) Energy and storage capacity (Ah)

FIGURE 7. Battery bank charging experimental results

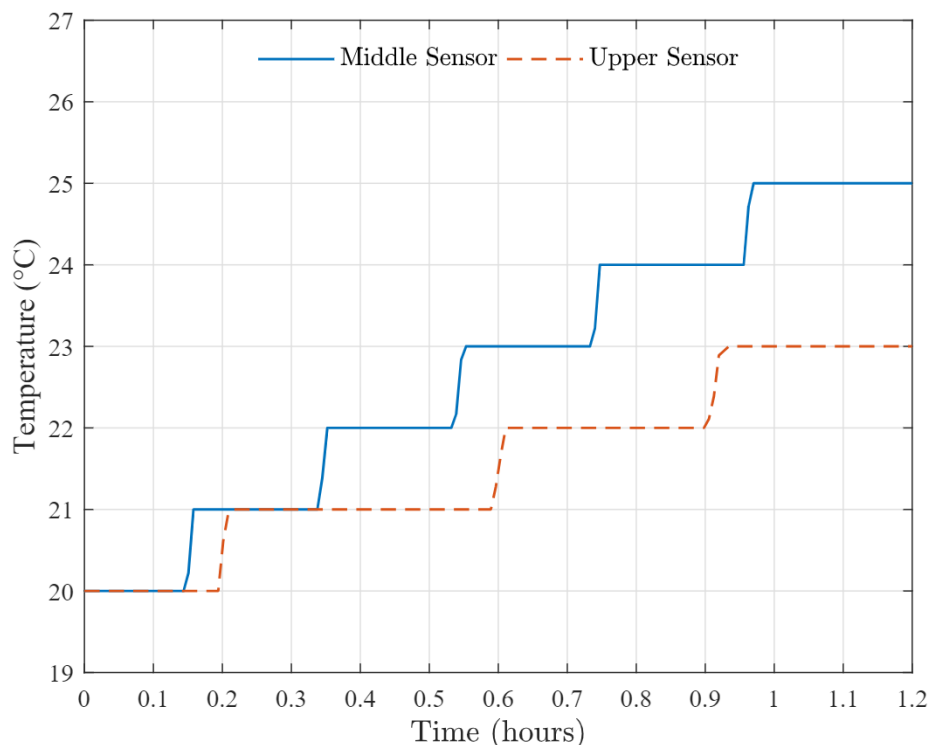


FIGURE 8. Thermal behavior of battery bank under 1C discharge

converters that allow the adaptation of the energy for the exoskeleton subsystems. The EMS proposed in this research has a capacity of 557 Wh, which permits autonomy of operation of the exoskeleton for at least one hour (1 h) under normal operating conditions.

Experimental results demonstrated effectiveness in the monitoring of critical variables of the battery pack (i.e., voltage, current, and temperature), as well as the voltage equalization procedure to get a minimum voltage difference of 0.01 V within the battery cells.

A power system represents more than just installing a battery pack in a device; as it was shown in the study presented in this paper, there are several functionalities that an energy system must include to guarantee portability. Future works to be developed by the authors include upgrading this design for applications related with unmanned ground vehicles (UGVs).

Acknowledgment. The authors are grateful for the support provided in this research by the Research Direction of University of Cuenca, under the financing of the project: “Robotic exoskeleton for functional assistance in walking patients with incomplete spinal cord injuries: design and initial application”.

REFERENCES

- [1] A. Rojas, A. Farfan, E. Mora, L. I. Minchala and S. Wong, Assessing the SNR influence in the estimation of the mean frequency of lower limbs sEMG signals, *IEEE Latin America Transactions*, vol.16, pp.2108-2114, 2018.
- [2] J. Li, G. Chen, P. Thangavel, H. Yu, N. Thakor, A. Bezerianos and Y. Sun, A robotic knee exoskeleton for walking assistance and connectivity topology exploration in EEG signal, *The 6th IEEE International Conference on Biomedical Robotics and Biomechanics (BioRob)*, pp.1068-1073, 2016.
- [3] P. Félix, J. Figueiredo, C. P. Santos and J. C. Moreno, Electronic design and validation of powered knee orthosis system embedded with wearable sensors, *2017 IEEE International Conference on Autonomous Robot Systems and Competitions (ICARSC)*, pp.110-115, 2017.

- [4] D. Astudillo, L. I. Minchala, F. Astudillo-Salinas, A. Vazquez-Rodas and L. Gonzalez, A simple mapping methodology of gait biomechanics for walking control of a biped robot, *2018 IEEE the 25th International Conference on Electronics, Electrical Engineering and Computing (INTERCON)*, pp.1-4, 2018.
- [5] L. I. Minchala, F. A. Salinas, K. P. Baus and A. V. Rodas, Mechatronic design of a lower limb exoskeleton, in *Mechatronic Systems in Engineering*, S. Yildirim (ed.), Rijeka, IntechOpen, 2017.
- [6] B. S. Rupal, S. Rafique, A. Singla, E. Singla, M. Isaksson and G. S. Virk, Lower-limb exoskeletons: Research trends and regulatory guidelines in medical and non-medical applications, *International Journal of Advanced Robotic Systems*, vol.14, no.6, 2017.
- [7] J. L. Pons, *Wearable Robots: Biomechatronic Exoskeletons*, John Wiley & Sons, 2008.
- [8] A. Kapsalyamov, P. K. Jamwal, S. Hussain and M. H. Ghayesh, State of the art lower limb robotic exoskeletons for elderly assistance, *IEEE Access*, vol.7, pp.95075-95086, 2019.
- [9] V. H. Duong, H. A. Bastawrous, K. C. Lim, K. W. See, P. Zhang and S. X. Dou, Online state of charge and model parameters estimation of the LiFePO₄ battery in electric vehicles using multiple adaptive forgetting factors recursive least-squares, *Journal of Power Sources*, vol.296, pp.215-224, 2015.
- [10] K. Brandt and J. Garche, General battery safety considerations, *Electrochemical Power Sources: Fundamentals, Systems, and Applications*, pp.1-19, 2019.
- [11] K. W. E. Cheng, B. P. Divakar, H. Wu, K. Ding and H. F. Ho, Battery-Management System (BMS) and SOC development for electrical vehicles, *IEEE Trans. Vehicular Technology*, vol.60, pp.76-88, 2011.
- [12] M. Hoque, M. Hannan, A. Mohamed and A. Ayob, Battery charge equalization controller in electric vehicle applications: A review, *Renewable and Sustainable Energy Reviews*, vol.75, pp.1363-1385, 2017.
- [13] S. Nogareda, *Determination of Energetic Metabolism through Tables*, Tech. Rep., National Institute of Occupational Safety and Hygiene, 2014.
- [14] C. Hall, A. Figueroa, B. Fernhall and J. A. Kanaley, Energy expenditure of walking and running: Comparison with prediction equations, *Medicine and Science in Sports and Exercise*, vol.36, pp.2128-2134, 2004.
- [15] E. Alcivar-Molina, J. Hurel, E. Terán, G. Zamora-Olea, R. Ponguillo and F. R. Loayza, Six-axis lower-limb exoskeleton control system based on neural networks, *2018 IEEE the 3rd Ecuador Technical Chapters Meeting (ETCM)*, pp.1-5, 2018.
- [16] M. Lelie, T. Braun, M. Knips, H. Nordmann, F. Ringbeck, H. Zappen and D. Sauer, Battery management system hardware concepts: An overview, *Applied Sciences*, vol.8, p.534, 2018.
- [17] K. Kandananond, The parsimonious and accurate characterization of an energy management system in hybrid vehicles based on statistical estimation methods, *ICIC Express Letters*, vol.14, no.2, pp.137-144, 2020.
- [18] S. B. Sarmah, P. Kalita, A. Garg, X.-D. Niu, X.-W. Zhang, X. Peng and D. Bhattacharjee, A review of state of health estimation of energy storage systems: Challenges and possible solutions for futuristic applications of Li-ion battery packs in electric vehicles, *Journal of Electrochemical Energy Conversion and Storage*, vol.16, 2019.